Two Photoluminescent Polymers Based on Fluorene and 2,4,6-Triphenyl Pyridine: Synthesis and Electroluminescence

Hong Ji Jiang,[1,2] Zhi Qiang Gao,[1] Xian Yu Deng,[1] Run Feng Chen,[1] Wei Huang[1]

[1]State Key Laboratory of Organic Electronics and Information Displays, Institute of Advanced Materials, School of Materials Science and Engineering, Nanjing University of Posts and Telecommunications, Nanjing 210046, China
[2]State Key Laboratory of Molecular Engineering of Polymers, Fudan University, Shanghai 200433, China

ABSTRACT: Two fluorene and triphenyl pyridine-based linear and dendronized copolymers, **P1** and **P2**, were synthesized and fully characterized by ^{1}H-NMR, ^{13}C-NMR, and matrix assistant laser desorption/ionization time-of-flight mass spectra, respectively. The absorption, photoluminescence (PL) behavior, and energy band gaps of **P1** and **P2** relative to those of polyfluorene end-capped with benzene (**P0**) were examined through UV–vis, photoluminescent spectra, and cyclic voltammetry. The UV–vis absorption and PL emission behavior of **P0** and **P1** were hardly affected by molecular architecture, while those of **P2** were strongly correlated with the dendronized molecular frameworks. Cyclic voltammetry studies indicated the lower highest occupied molecular orbital energy level and wider band gap of **P2** thin solid film relative to those of **P0** and **P1**. The new polymers were thermally stable up to 410°C. The better luminance and external quantum efficiencies of **P1** relative to those of **P0** in polymer light-emitting diode (PLED) applications are due to improved electron injection, charge trapping and recombination at the pyridine sites. Through the experiments, it is found that the triphenyl pyridyl segments and excimers-formation make pronounced contribution to long wavelength emission in **P1**-based blue light-emitting materials, and the analogous materials containing 2,4,6-triphenyl pyridyl unit of **P1** constitute highly attractive materials for white PLED applications. © 2011 Wiley Periodicals, Inc. J Appl Polym Sci 124: 3921–3929, 2012

Key words: polymer light-emitting diode; pyridine; electroluminescent; long wavelength emission

INTRODUCTION

As one of the important blue emissive materials, fluorene and its derivatives have drawn much attention of material chemists and device physicists in organic semiconductor field due to their aromatic biphenyl structure, wide energy band gap, and high luminescent efficiency.[1,2] So far, the most intensely studied polymers are linear conjugated π-systems, which are prone to aggregate and end up with self-quenching of their luminescence.[3–10] Therefore, preparation and investigation of polyfluorenes (**PF**s) with dendronized structure is emerging.[11–14] Such materials are expected to be less aggregated and should not suffer from photoluminescence (PL) quenching due to the weak intermolecular interactions. However, it is thought that the current understanding of **PF**s with dendronized molecular architecture is not sufficient, and the optoelectronic properties of conjugated polymers vary significantly considering the degree of extended conjugation between the consecutive repeating units and the inherent electron densities on the polymer backbone. Therefore, there is a need to investigate the fine electro-optical difference of **PF**s. To fulfill this objective, many strategies could be envisaged to diversify the structure of **PF**s. The most common one implies the diversification of the parent skeletons of polymers. Pyridine has been a key building block in constructing functional materials in view of its outstanding mechanical and dielectric properties.[15–17] Since, they can harvest both

singlet and triplet excitons, enabling internal quantum efficiencies close to 100%, the attention in most reports about the pyridine building block in polymer light-emitting diode (PLED) application has been paid to the electrophosphorescent metal complexes,[18] and the report about **PF**s containing pyridyl moiety with different molecular architecture is still rare.[19] Generally, PLED fabricated from **PF**s derivatives suffer from the degradation under operation, that is, the formation of a low-energy emission band at 500–600 nm and the blue emission being evolved into the unwanted blue-green emission. So far, different models have been proposed to explain the origin of the green emission from **PF**s derivatives.[20–25] Some think that the dendronized **PF**s can eliminate the long-wavelength emission in some degree, while others claim that the linear **PF**s with bulky side groups can be a more competitive one.[26] To the best of our knowledge, there are rare reports about the correlation between the electro-optical properties and linear or dendronized **PF**s molecular structure.[27] In this context, further investigations are needed to overcome this problem through suitable synthetic strategies.

Our research efforts have long focused on the synthesis and structure-property investigations of nonplanar conjugated polymers for long term.[28] We have synthesized polymers having sterically hindered side chains, and the electro-optical properties of wide band gap noncoplanar copolymers are tunable by the sterically hindered pyridine moieties.[29] In this contribution, to gain a deep insight into the correlation between the molecular architecture and the electro-optical properties of linear or dendronized polymers, we present the synthesis of two fluorene and triphenyl pyridine-based copolymers, **P1** and **P2**, and some interesting electro-optical varieties regarding the contribution of 2,4,6-triphenylpyridine to the photophysical, electrochemical, and the long wavelength emission of **PF**-based blue polymers are obtained and discussed.

EXPERIMENTAL

Materials and characterization

Fluorene, *n*-butyl-lithium, 2,7-dibromo-fluorene, 2-bromo-fluorene, 4-bromo-benzaldehyde, 1-(4-bromophenyl) ethanone, acetophenone, triisopropyl borate, and tetrakis (triphenylphosphine) palladium(0) (Pd(PPh₃)₄) were purchased from Acros Organics and used without further purification. Tetrahydrofuran (THF) and toluene were distilled over sodium/benzophenone under nitrogen atmosphere. The other common solvents were treated according to the standard method.

All NMR spectra were recorded on a Varian Mercury plus 400 at 295 K. The thermal gravimetric analysis (TGA) scan was done on Shimadzu DTG-60A equipment with a heating rate of 10°C/min and nitrogen as the purge gas. The ultraviolet-visible (UV–vis) absorption and PL emission spectra were recorded on Shimadzu UV-3150 and RF-5300PC spectrometers, respectively. The molecular masses of intermediates were determined by Shimadzu Matrix assistant laser desorption/ionization time-of-flight mass spectrometry (MALDI-TOF-MASS). The gel permeation chromatography (GPC) measurements were performed on a Shimadzu LC10A chromatograph with THF as eluent and polystyrenes as external standards. The absolute PL quantum yields were determined using thin films in integrated sphere with a laser of 374 nm at room temperature. Cyclic voltammetry (CV) was performed on an AUTOLAB PGSTAT30 potentiostat/galvanostat system (Ecochemie, Netherlands).

The PLEDs were fabricated on prepatterned indium-tin oxide (ITO). The substrate was ultrasonically cleaned with acetone, detergent, deionized water, and 2-propanol. Oxygen plasma treatment was made for 4 min as the final step just before the film coating. Onto the ITO glass was spin-coated a layer of polyethylenedioxythiophene-polystyrene sulfonic acid (PEDOT : PSS) film with thickness of 40 nm from its aqueous dispersion as the hole injection and transport layer. The PEDOT : PSS film was dried at 80°C for 3 h in the vacuum oven. The solution of polymers in toluene was prepared under nitrogen atmosphere and spin-coated on to PEDOT : PSS layer. Typical thickness of the emitting layer was 100 nm. Then a thin layer of barium as an electron injection cathode and the subsequent 150 nm thick aluminum protection layers were thermally deposited by vacuum evaporation through a mask at a base pressure below 2×10^{-4} Pa. The cathode area defined the active area of the device. The typical active area of the devices in this study was 0.15 cm². The electroluminescent (EL) layer spin coating process and the device performance tests were carried out within a glove box under a nitrogen atmosphere. The luminance of the device was measured with a calibrated photodiode. External quantum efficiency was verified by the measurement of the integrating sphere, and luminance was calibrated after the encapsulation of devices with UV-curing epoxy and thin cover glass.

The monomers of 2,7-bis(trimethylene boronate)-9,9-dioctylfluorene(**1**),[20] 2,7-dibromo-9,9-dioctylfluorene(**2**),[20] 2,4,6-tris(4-bromophenyl)pyridine(**3**),[29] and 2,6-bis(4-bromophenyl)-4-phenyl pyridine(**4**)[29] were synthesized according to documented procedures.

3.¹H-NMR (400 MHz, CDCl₃): δ (ppm) = 7.63−7.65 (m, 8H), 7.80−7.81 (s, 2H), 8.03−8.06 (d, 4H). ¹³C-
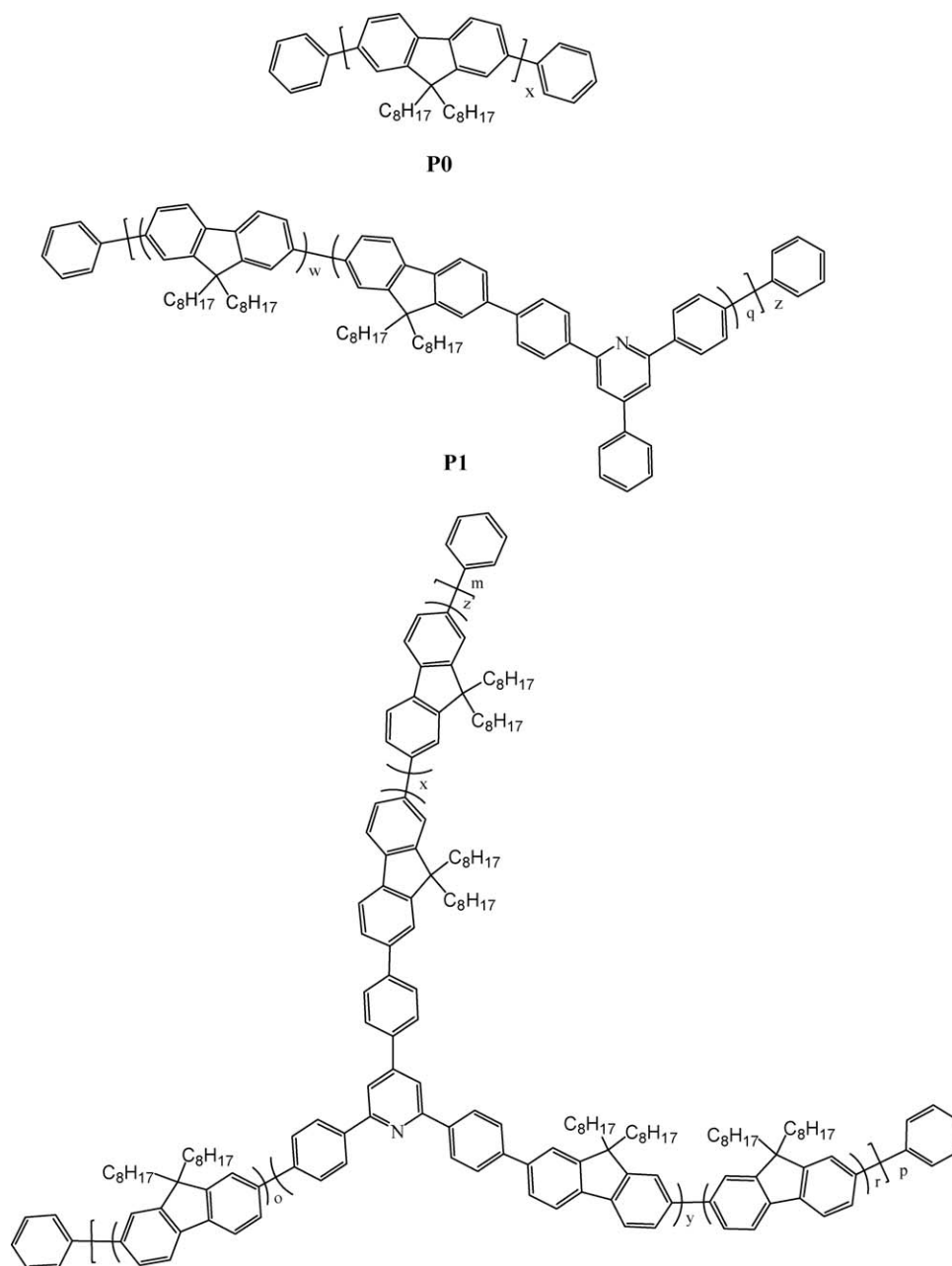
**Scheme 1** Chemical structure of polymers **P0**, **P1**, and **P2**.

NMR (100 MHz, CDCl$_3$): δ (ppm) = 116.992, 124.029, 128.856, 132.616, 138.125, 129.856, 196.848. MS (MALDI-TOF-MASS): m/z = 543.60 (M$^+$).

4.^{1}H-NMR (400 MHz, CDCl$_3$): δ (ppm) = 7.43–7.60 (m, 3H), 7.60–7.70 (m, 4H), 7.70–7.79 (m, 2H), 7.83–7.93 (s, 2H), 8.002–8.122 (s, 4H). ^{13}C-NMR (100 MHz, CDCl$_3$): δ (ppm) = 117.438, 123.919, 127.423, 128.908, 129.450, 129.466, 132.130, 138.430, 138.81, 150.91, 156.61. MS (MALDI-TOF-MASS): m/z = 465.60 (M$^+$).

Poly(2,7-diyl-9,9-dioctylfluorene) (P0)

A mixture of **1** (0.77 g, 1.37 mmol), **2** (0.76 g, 1.37 mmol), alq336, and catalytic amount of Pd(PPh$_3$)$_4$ was added to a degassed mixture of toluene (20 mL) and Na$_2$CO$_3$ aqueous solution (2M, 4 mL). The mixture was vigorously stirred at 90°C for 72 h under a nitrogen atmosphere. After the routine end-capping reaction of 1-bromobenzene and phenylboronic acid, 150 mL toluene was added, and the organic layer was separated and washed with brine for drying over anhydrous MgSO$_4$. The residue was purified with a short column chromatography on silica gel with toluene as eluent to yield the light yellow solution. Upon part of solvent being evaporated off, the concentrated solution was dropped slowly into a solution of methanol while being well stirred. The obtained organic precipitate was collected on a filter,
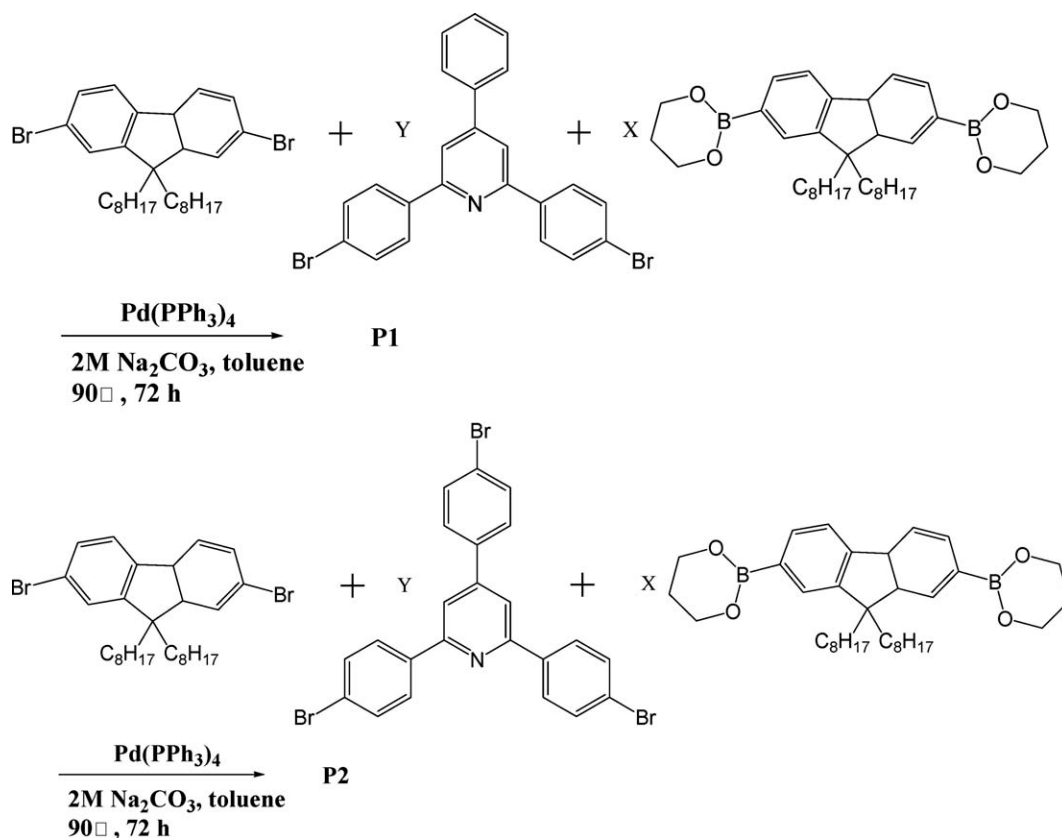
Scheme 2 Synthetic route of polymers **P1** and **P2**.

washed with methanol followed by soxhlet extraction with acetone for 48 h to remove the oligomers and catalyst residue. The recovered yield of the yellow solid was 73%.

**Poly((2,7-diyl-9,9-dioctylfluorene)-*co*-
(2,6-bi(4-phenyl)-4-phenyl pyridine)) (P1) and
Poly((2,7-diyl-9,9-dioctylfluorene)-*co*-(2,4,6-tris
(4-phenyl) pyridine)) (P2)**

P1 and **P2** were synthesized similarly according to the procedure to prepare **P0**.

P1

1 (0.77 g, 1.37 mmol), **2** (0.55 g, 1 mmol), **4** (0.17 g, 0.37 mmol), toluene (20 mL), and Na_2CO_3 aqueous solution (2M, 4 mL). ^{1}H-NMR (400 MHz, CDCl$_3$,): δ (ppm) = 0.96–0.50 (broad), 1.43–0.97 (broad), 2.40–1.89 (s), 7.60–7.44 (broad), 7.71–7.60 (broad), 7.96–7.78 (broad), 8.102–7.97 (s), 8.49–8.28 (s). ^{13}C-NMR (100 MHz, CDCl$_3$): δ (ppm) = 14.172, 22.70, 24.14, 29.46, 30.27, 32.12, 40.63, 55.57, 120.20, 121.83, 126.39, 127.44, 129.01, 140.24, 140.71, 152.03.

P2

1 (0.77 g, 1.37 mmol), **2** (0.55 g, 1 mmol), **3** (0.14 g, 0.25 mmol), toluene (20 mL), and Na_2CO_3 aqueous solution (2M, 4 mL). ^{1}H-NMR (100 MHz, CDCl$_3$): δ (ppm) = 0.38–1.47 (broad), 1.87–2.69(s), 7.31–8.22 (broad), 8.51–8.31(s). ^{13}C-NMR (100 MHz, CDCl$_3$): δ (ppm) = 14.159, 22.72, 24.08, 29.36, 30.26, 32.01, 40.56, 55.57, 120.18, 121.71, 126.26, 127.35, 128.98, 140.24, 140.70, 152.03.

RESULTS AND DISCUSSION

Synthesis and characterization of the polymers

Polymers **P0**, **P1,** and **P2** were prepared easily by the Suzuki coupling method using **1** and **2**, **3**, **4** at different feeding ratios (Schemes 1 and 2). Since it had been well established that the monomer with multifunction tended to produce insoluble cross-linked polymers in the step-growth polymerization, therefore, the Suzuki coupling reaction was much better to be carried out in a dilute solution and relatively low temperature to reduce the possible cross-linking between branches to avoid the poor solubility of **P2**. The amount of **3** with multifunction to synthesize **P2** was controlled to some degree, and the molar ratio of **4** in **P1** was adjusted to be one and a half of that of **3** for comparison. The whole Suzuki coupling reaction was controlled utmost to be parallel. All polymers were finally end-capped with benzene to improve thermal stability. **P0** and

P1 were completely soluble in common organic solvents, such as chloroform, toluene, and ethyl acetate at room temperature. P2 could only be soluble in chloroform and toluene, and be partly soluble in THF or dichloromethylene, which indicated that it was of dendronized structure rather than crosslinked one. The weight-average molar mass (M_w) of P0, P1, and P2 was 8100, 10,400, and 73,700 with the polydispersity (PDI) of 1.27 (monomodal), 1.22 (monomodal), and 5.4 (multimodal). The molecular weight and PDI of P2 were much higher than those of P0 and P1, which could be attributed to the multifunctional monomer of 3. TGA studies on polymers P0, P1, and P2 revealed high thermal stability with decomposing temperature above 410°C at 5% weight loss (see Supporting Information). However, we can determine from NMR calculation that the average ratios of fluorene to triphenyl pyridine in obtained polymer P1 and P2 are 4.83 and 6.3 from the number of o-position phenyl hydrogen of the pyridine and the methane adjacent to the 9-position of fluorene (see Supporting Information), which is lower than the original feeding ratio in some degree.

Photophysical properties

The photophysical properties of P0, P1, and P2 were investigated both in THF solution and in thin solid films. The absorption and PL emission data for the polymers was summarized in Figures 1, 2 and Table I. As shown in Figures 1 and 2, the absorption spectra of the polymer solutions and thin films were very similar in a range of 369–384 and 375–399 nm, respectively, which could be attributed to the π-π* transitions of the polymers. The absorption maximum in THF solution underwent a blue shift with the increase of the branched degree in the turn of P0, P1, and P2, which illustrated that there existed
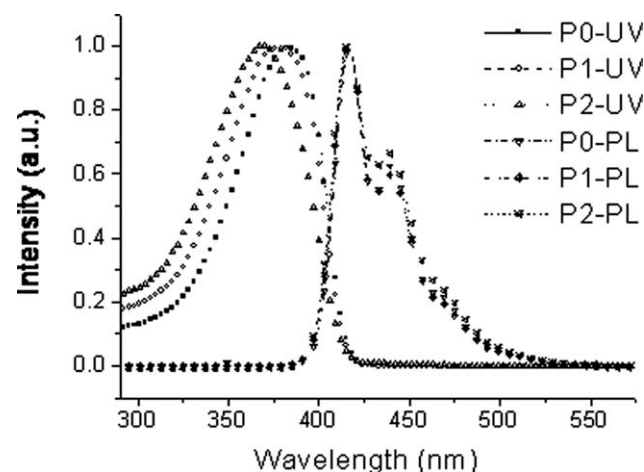

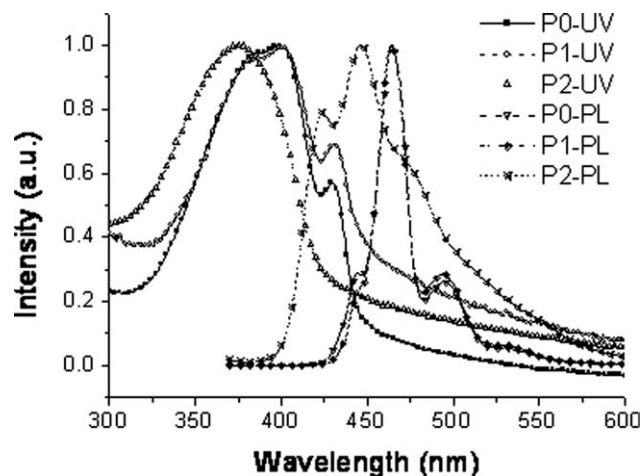**Figure 1** Normalized UV–vis absorption and PL emission spectra of P0, P1, and P2 in THF solution.

Figure 2 Normalized UV–vis absorption and PL emission spectra of P0, P1, and P2 in thin solid films.

some different conjugated structures of polymers in highly dilute solution. The incorporation of 2,4,6-triphenyl pyridyl linkages to main chain of PFs has arisen the interruption of the delocalization of π-electrons along the polymer backbones. However, as evaluated from the onsets of the film absorption spectra, the optical band gaps of these polymers in solution were all 3.01 eV. This indicated that the optical band gap was mainly dominated by the oligofluorene segments in the main chain of polymers. The similar emissions observed for these copolymers in comparison with that of PFs homopolymer in dilute solution suggested that the triphenyl pyridyl derivatives in the polymer backbones did not prevent efficient energy transfer from the short conjugated emissions to the long ones in these copolymers. Figure 2 showed the UV–vis absorption and PL emission spectra of the polymers in thin films. Unlike the behaviors in THF solution, the UV–vis absorption and PL emission spectra of P2 in thin film exhibited a slight blue shift, due to the increase of energy band gap relative to those of P0 and P1, while those of P0 and P1 kept approximately equivalent at 399 nm, respectively, and shouldered around

TABLE I
Polymerization Results, Molecular Weights, and Thermal Data of Polymers

Polymer	Yield (%)	M_n ($\times 10^4$)[a]	M_w ($\times 10^4$)[a]	PDI[b]	TGA (°C)[c]
P0	75	0.64	0.81	1.27	436
P1	62	0.85	1.04	1.22	417
P2	50	1.36	7.37	5.4	420

[a] Determined by GPC in THF based on polystyrene standards.
[b] Polymer Distribution Index (PDI).
[c] Temperature at 5% weight loss under nitrogen at a scan rate of 10°C/m.

TABLE II
Photophysical Properties of the Polymers P0, P1, and P2

	THF			Film			
	λ_{max}^{abs} (nm)[a]	$\lambda_{max}^{em/ex}$ (nm)[b]	E_g^{opt} (eV)[c]	λ_{max}^{abs} (nm)[a]	$\lambda_{max}^{em/ex}$ (nm)[b]	E_g^{opt} (eV)[c]	Q_{pl} (%)[d]
P0	384	416 (370)	3.01	399	464 (354)	2.80	48.3
P2	381	417 (372)	3.04	399	464 (356)	2.78	24.0
	369	416 (373)	3.03	375	446 (358)	2.87	6.8

[a] Maximum absorption wavelength.
[b] Maximum emission and excitation wavelength.
[c] Optical band gap determined from the UV–vis absorption onset.
[d] Absolute PL quantum efficiency of thin solid films.

430 nm. However, it was clear that both polymers P0 and P1 aggregated in films. The blue shift in absorption and emission observed for P2 was therefore very likely due to a decreased aggregation resulted from the dendronized architecture of P2. The additional absorption shoulder around 430 nm in film of P0 and P1 was related to the β-phase,[30] which is not seen in the absorption spectra of P2 films, and the highly dendronized structure of P2 made the molecule not easy to form planar conjugated structure. The PL spectra of the polymer solutions exhibited similar vibronic features with a narrow bandwidth and emission maxima at around 416–436 and 450–490 nm. In general, the presence of well-defined vibronic features in the emission spectra indicated that the polymer had a rigid and well-defined backbone structure.[31,32] Both P1 and P2 exhibited two main emissions, and this emission maximum was clearly not dependent of the excitation wavelength. This further indicated the existence of possible efficient energy transfer among the segments with different conjugated length.[33]

To assess the effect of molecular architecture on the capability of polymers for light-emitting, the absolute PL quantum yields of polymer thin solid films were determined by using films in integrated sphere with a laser of 374 nm at room temperature. It was interesting in that the absolute PL quantum efficiencies of films were as high as 48.3% for P0, 24.0% for P1, and 6.8% for P2. Generally, a material with high PL quantum efficiency should have one of the following characteristics: big rigid planar π-conjugated structure, electron-rich substitutions and the lowest single excitation level of π-π*[34–36]. In the turn of P0, P1, and P2, the absolute PL quantum yields were gradually decreased, which was in agreement with the increase of the branched level of polymers. The aggregates among molecules could strongly affect the PL properties of conjugated polymers by red-shifting their fluorescence spectra and lowering PL quantum efficiency.[37] However, the more nonplanar moieties of triphenyl pyridine in P2 were thought enough for impeding π-stacking aggregation

and intermolecular excimer formation, which was related to the improvement of the overall external quantum efficiency of PLED. The kinked molecular structures of P1 and P2 made it difficult to form intermolecular stacking, which prevented aggregation of the polymer main chains, thereby reducing the PL quenching, and in turn were expected to increase the absolute PL quantum yields, but the results were just reverse. The copolymers P1 and P2 showed decreased PL efficiencies compared with homopolymer P0,[38] and an explanation of the evolution of the absolute PL quantum yields in the series P0, P1, to P2 could be that the triphenyl pyridine moieties might serve as efficient quenching site either because they inherently quench excitons or because they are possible sites for structural defects.[39,40]

Electrochemical properties

To provide further proof for the photophysical properties of polymers, we employed CV to evaluate the highest occupied molecular orbital (HOMO) and lowest unoccupied molecular orbital (LUMO) energy levels of P0, P1, and P2 films. The oxidation and reduction potentials derived from the onset of electrochemical potential were summarized in Table II, and Figure 3 illustrated the CV curves in details. All polymers exhibited complete reversibility both in p-doping and n-doping processes, suggesting the potential for bipolar charge transport properties. The HOMO and LUMO energy levels of P0 and P1 were −5.80 and −2.20 eV, and the corresponding band gaps were 3.6 eV,[41–45] which further validated that the energy band gap of P1 was mainly dominated by the oligofluorene segments in the polymers. With the further increase of branched degree to P2, the oxidation potential was considerably changed, which made the HOMO and LUMO energy levels of P2 films to be −6.05 and −2.19 eV. The HOMO energy level of P2 was reduced and the band gap was increased to be 3.86 eV. On account of the fact that the triphenyl pyridine in P1 did not obviously
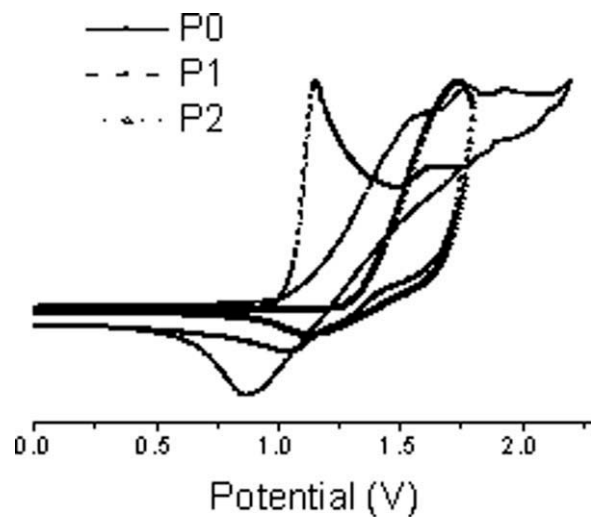
(a)
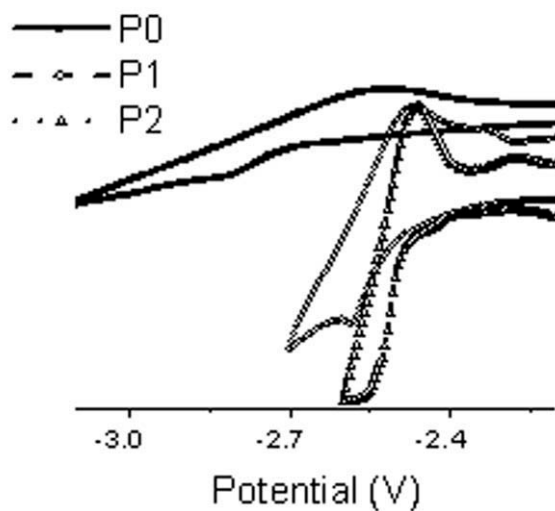
(b)

Figure 3 CV curves of **P0**, **P1**, and **P2** films.

Figure 4 EL emission spectra of **P0** and **P1** with a device structure of D1.

change the HOMO and LUMO energy levels of parent backbone in film, the above abnormal HOMO energy level of **P2** films could only attribute to the dendronized structure. The lower HOMO energy level of **P2** films made it potential hole-blocking material relative to that of **P0** and **P1**.

EL properties

Owing to the relative high PL efficiency of **P0** and **P1**, the applications of polymers **P0** and **P1** as emitting layers in PLEDs were investigated in a ternary-layer device with the following configuration (D1): ITO/PEDOT : PSS(40 nm)/PVK(40 nm)/**PX**(80 nm)/ Ba(4 nm)/Al(130 nm). The EL spectra and results are illustrated in Figures 4 and 5, respectively. Here, PEDOT doped with PSS was used as the hole
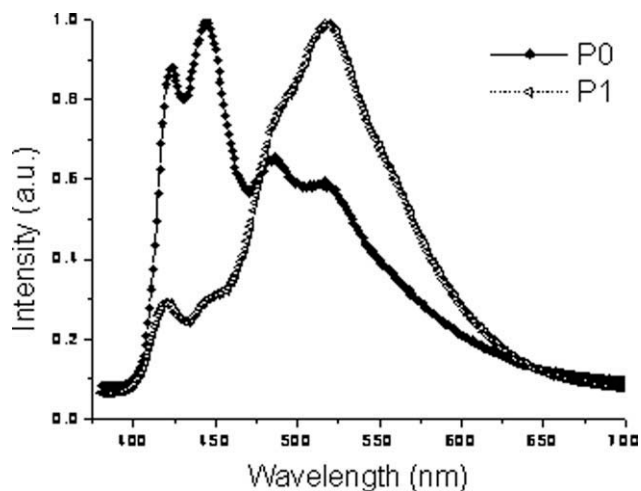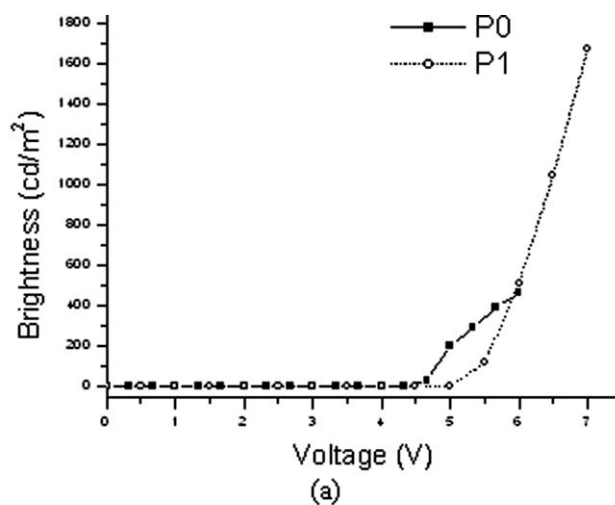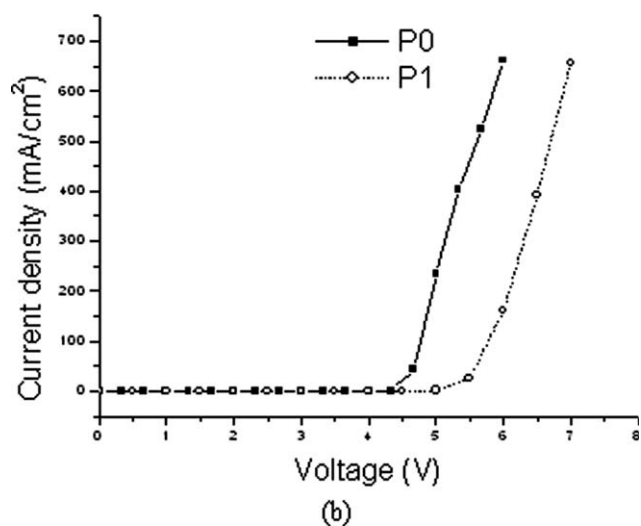

(a)

(b)

Figure 5 Voltage-luminance (a) and voltage-current density characteristics (b) of **P0** and **P1**.

TABLE III
Eectrochemical Data of the Polymers P0, P1, and P2

Polymer	Reduction[a] E_{pa}/E_{pc} (V)[e]	Oxidation[a] E_{pc}/E_{pa} (V)[e]	LUMO/ HOMO (eV)[b]	E_g^{cv} (eV)[c]	E_g^{opt} (eV)[d]
P0	−2.54/−2.80	1.78/0.87	−2.19/−5.82	3.63	2.78
P1	−2.46/−2.53	1.06/1.15	−2.21/−5.79	3.58	2.76
P2	−2.30/−2.40	1.14/1.71	−2.19/−6.05	3.86	2.91

[a] Determined by cyclic voltammetry of polymer films coated on glassy carbon electrodes in fresh distilled acetonitrile with Ag/AgNO3 (0.1M) as a reference electrode. Scan rate: 100 mV s^{-1}.

[b] HOMO and LUMO energy levels were calculated with reference to ferrocene (4.7 eV).

[c] Electrochemical band gap obtained by cyclic voltammetry.

[d] Optical band gap determined from the UV–vis absorption onset in thin solid film.

[e] E_{pa} and E_{pc} stood for anodic peak potential and cathodic peak potential, respectively.

injection layer, and PVK was used as a hole transporting and electron-blocking material in OLEDs (Table III). The PLEDs exhibit onset voltages of 3.9 V for **P0** and 5.8 V for **P1**, maximum brightness of 481 cd/cm^2 at a voltage of 6 V for **P0** and 1685 cd/cm^2 at a voltage of 9 V for **P1**, and external quantum efficiency of 0.15% for **P0** and 0.3% for **P1**. We find an obvious long-wavelength emission locating at 538 nm in the EL spectra of **P0**, which matches exactly with the previously reported troublesome green EL band in blue emitting **PF**s. The EL spectra of **P1** have completely evolved into white light emission (CIE = 0.25, 0.28), and the blue emission is quenched completely. Since the long-wavelength broad peaks at 520 nm in the EL spectra of **P1** are very close to the location of the longer-wavelength shoulders in the PL spectra of the **PF** films, the longer-wavelength emissions in the EL spectra of **P1** should result from excimers.[46] However, the fact that this emission is also seen in PL emission spectra of **P0** and **P1** films, and the reduced PL quantum efficiency of **P1** and **P2** films suggests that it does not originate solely from intermolecular aggregates or excimers,[47] and the low-energy pyridyl moieties on the main chain of **P1** may act as deep traps to carriers. It is interesting that the analogous oxidized phosphorus atom on phosphafluorene significantly changes the blue electroluminescence of **PF** into white PLED,[38] while carbazole-substituted aromatic enynes can act as an excellent single-emitting component for white PLEDs as a combination of the blue emission from an isolated molecule with the longer-wavelength emissions from excimers.[46] In this regard, the analogous triphenyl pyridyl segments and excimers may cause the white light emission in the EL spectra of **P1**, and the analogous materials of **P1** can be a good alternative for white light PLED application.[48] Further improvements of the devices based on these materials will include the optimization of the chemical composite of **P1** and the precise control of the morphology of the films to obtain white light PLED with high color purity and stability.

CONCLUSIONS

Two polymers with diverse molecular architecture were synthesized, and the effect of molecular architecture on the photophysical and EL properties of these materials were investigated. The experimental results demonstrated that UV–vis absorption and PL emission behavior of **P0** and **P1** were hardly affected by molecular architecture, while those of **P2** were strongly correlated with the dendronized molecular frameworks. The better luminance and external quantum efficiencies of **P1** relative to those of **P0** in PLED applications are due to improved electron injection, charge trapping, and recombination at the pyridine sites. Through the EL experiments, it is found that the analogous materials of **P1** can be a good choice for white light PLED applications.

References

1. Burroughes, J. H.; Bradley, D. D. C.; Brown, A. R.; Marks, R. N.; Friend, R. H.; Burn, P. L.; Holmes, A. B. Nature 1990, 347, 539.
2. Wong, W.; Liu, Y. L.; Cui, D. M.; Leung, L. M.; Kwong, C. F.; Lee, T. H.; Ng, H. F. Macromolecules 2005, 38, 4970.
3. Marsitzky, D.; Vestberg, R.; Blainey, P.; Tang, B. Y.; Hawker, C. J.; Carter, K. R. J Am Chem Soc 2001, 123, 6965.
4. Pogantsch, A.; Wenzl, F. P.; List, E. J. W.; Leising, G.; Grimsdale, A. C.; Müllen, K. Adv Mater 2002, 14, 1061.
5. Evans, N. R.; Devi, L. S.; Mak, C. S. K.; Watkins, S. E.; Pascu, S. I.; Köhler, A.; Friend, R. H.; Williams, C. K.; Holmes, A. B. J Am Chem Soc 2006, 128, 6647.
6. Beaupre, S.; Ranger, M.; Leclerc, M. Macromol Rapid Commun 2000, 21, 1013.
7. Craig, M. R.; Dekok, M. M.; Hofstraat, J. W.; Schenning, A. P. H. J.; Meijer, E. W. J Mater Chem 2003, 13, 2861.
8. Kulkarni, P.; Jenekhe, S. A. Macromolecules 200336, 5285.
9. Chochos, C. L.; Tsolakis, P. K.; Gregoriou, V. G.; Kallitsis, J. K. Macromolecules 2004, 37, 2502.

10. Surin, M.; Hennebicq, E.; Ego, C.; Marsitzky, D.; Grimsdale, A. C.; Müllen, K.; Bredas, J. L.; Lazzaroni, R.; Leclere, P. Chem Mater 2004, 16, 994.
11. List, E. J. W.; Guntner, R.; Scandiuccide, F. P.; Scherf, U. Adv Mater 2002, 14, 374.
12. Sims, M.; Bradley, D. D. C.; Ariu, M.; Koeberg, M.; Asimakis, A.; Grell, M.; Lidzey, D. G. Adv Funct Mater 2004, 14, 765.
13. Li, Y. N.; Ding, J. F.; Day, M.; Tao, Y.; Lu, J. P.; D'iorio, M. Chem Mater 2003, 15, 4936.
14. Liu, J. G.; Wang, L. F.; Yang, H. X.; Li, H. S.; Li, Y. F.; Fan, L.; Yang, S. Y. J Polym Sci Part A: Polym Chem 2004, 42, 1845.
15. Wang, R. Y.; Jia, W. L.; Aziz, H.; Vamvounis, G.; Wang, S.; Hu, N. X.; Popovic, Z. D.; Coggan, J. A. Adv Funct Mater 2005, 15, 1483.
16. Chen, S. Y.; Xu, X. J.; Liu, Y. Q.; Yu, G.; Sun, X. B.; Qiu, W. F.; Ma, Y. Q.; Zhu, D. B. Adv Funct Mater 2005, 15, 1541.
17. Pan, X. Y.; Liu, S. P.; Chan, H. S. O.; Ng, S. C. Macromolecules 2005, 18, 7629.
18. Zhen, H. Y.; Jiang, C. Y.; ; Yang, W.; Jiang, J. X.; Huang, F.; Cao, Y. Chem Eur J 2005, 17, 5007.
19. Yang, J. X.; Tao, X. T.; Yuan, C. X.; Yan, Y. X.; Wang, L.; Liu, Z.; Ren, Y.; Jiang, M. H. J Am Chem Soc 2005, 127, 3278.
20. Zhou, X. H.; Zhang, Y.; Xie, Y. Q.; Cao, Y.; Pei, J. Macromolecules 2006, 39, 3830.
21. Xin, Y.; Wen, G. A.; Zeng, W. J.; Zhao, L.; Zhu, X. R.; Fan, Q. L.; Feng, J. C.; Wang, L. H.; Wei, W.; Peng, B.; Cao, Y.; Huang, W. Macromolecules 2005, 38, 6755.
22. Li, J.; Li, M.; Bo, Z. S. Chem Eur J 2005, 11, 6930.
23. Chen, X. W.; Tseng, H. E.; Liao, J. L.; Chen, S. A. J Phys Chem B 2005, 109, 17496.
24. Hung, M. C.; Liao, J. L.; Chen, S. A.; Chen, S. H.; Su, A. C. J Am Chem Soc 2005, 127, 14576.
25. Chi, C. Y.; Im, C.; Enkelmann, V.; Ziegler, A.; Lieser, G.; Wegner, G. Chem Eur J 2005, 11, 6833.
26. Yang, X. H.; Jaiser, F.; Neher, D.; Lawson, P. V.; Brédas, J. L.; Zojer, E.; Güntner, R.; Scanduicci, de Freitas, P.; Forster, M.; Scherf, U. Adv Funct Mater 2004, 14, 1097.
27. Vak, D.; Lim, B.; Lee, S. H.; Kim, D. Y. Org Lett 2005, 7, 4229.
28. Lai, W. Y.; He, Q. Y.; Zhu, R.; Chen, Q. Q.; Huang, W. Adv Funct Mater 2008, 18, 265.
29. Jiang, H. J.; Gao, Z. Q.; Liu, F.; Ling, Q. D.; Wei, W.; Huang, W. Polymer 2008, 49, 4369.
30. Ariu, M.; Sims, M.; Rahn, M. D.; Hill, J.; Fox, A. M.; Lidzey, D. G.; Oda, M.; Cabanillas-Gonzalez, J.; Bradley, D. D. Phys Rev B: Solid State 2003, 67, 195333.
31. Wu, W.; Tsai, C. C. M.; Lin, H. C. Macromolecules 2006, 39, 4298.
32. Taranekar, P.; Abdulbaki, M.; Krishnamoorti, R.; Phanichphant, S.; Waenkaew, P.; Patton, D.; Fulghum, T.; Advincula, R. Macromolecules 2006, 39, 3848.
33. Peng, Q.; Peng, J. B.; Kang, E. T.; Neoh, K. G.; Cao, Y. Macromolecules 2005, 38, 7292.
34. Ding, J.; Day, M.; Robertson, G.; Roovers, J. Macromolecules 2002, 35, 3474.
35. Mishra, A. K.; Graf, M.; Grasse, F.; Jacob, J.; List, E. J. W.; Müllen, K. Chem Mater 2006, 18, 2879.
36. Huang, C. H.; Li, F. Y.; Huang, Y. Y. Ultrathin Films for Optics and Electronic, 1st ed.; Beijing University Publishing House: Bei Jing 2001, 159.
37. Peng, K. Y.; Chen, S. A.; Fan, W. S. J Am Chem Soc 2001, 123, 11388.
38. Chen, R. F.; Zhu, R.; Fan, Q. L.; Huang, W. Org Lett 2008, 10, 2913.
39. Ma, Z.; Lu, S.; Fan, Q. L.; Qing, C. Y.; Wang, Y. Y.; Wang, P.; Huang, W. Polymer 2006, 47, 7382.
40. Osaheni, J. A.; Jenekhe, S. A. Macromolecules 1994, 27, 739.
41. Chochos, C. L.; Kallitsis, J. K.; Gregoriou, V. G. J Phys Chem B 2005, 109, 8755.
42. Jaramillo-Isazaab, F.; Turner, M. L. J Mater Chem 2006, 16, 83.
43. Hou, J. H.; Yang, C. H.; He, C.; Li, Y. F. Chem Commun 2006, 8, 871.
44. Jiang, H. J.; Wang, H. Y.; Feng, J. C.; Wang, C. M.; Fan, Q. L.; Wei, W.; Huang, W. J Polym Sci Part A: Polym Chem 2006, 44, 4346.
45. Zhu, R.; Wen, G. A.; Feng, J. C.; Chen, R. F.; Zhao, L.; Yao, H. P.; Fan, Q. L.; Wei, W.; Peng, B.; Huang, W. Macromol Rapid Commun 2005, 26, 1729.
46. Liu, Y.; Nishiura, M.; Wang, Y.; Hou, Z. M. J Am Chem Soc 2006, 128, 5592.
47. Kulkarni, A. P.; Kong, X. X.; Jenekhe, S. A. J Phys Chem B 2004, 108, 8689.
48. Chan, K. L.; Sims, M.; Pascu, S. I.; Ariu, M.; Holmes, A. B.; Bradley, D. D. C. Adv Funct Mater 2009, 19, 2147.